CHAPTER-2

Theoretical background and experimental methods

2.1 Theories of liquid crystalline phases:

The theories of liquid crystalline phase have been described in detail in several books of which some are listed in the references [1-5]. In present work I have tried to compare the experimental values of the order parameters of nematics and smectics with those obtained from Maier-Saupe mean field theory and McMillan theory respectively. As such I have discussed, in short, Maier Saupe mean field theory [6] and McMillan theory [7,8] respectively.

2.2 Maier-Saupe mean field theory of nematic phase of rod like molecules:

Maier and Saupe have given a molecular statistical theory of the nematic phase with one order parameter. Suppose that the liquid crystal is composed of rod-like molecules in which the long axis of the molecules tend to align parallel to the director **n** in mesophase. The stability of the nematic liquid crystal phase arises from the existence of the anisotropic part of the dispersion interaction energy between the molecules. This energy originates from the intermolecular electrostatic interaction. For the sake of simplicity Maier and Saupe approximated the electrostatic interaction by the first term of its multipole expansion and assumed that:

a/ the influence of the permanent dipoles can be neglected as far as long range nematic order is concerned.

b/ only the effect of the induced dipole-dipole interaction need to be considered.

c/ the molecules may be considered to be cylindrical symmetric about its long axis.

d/ with respect to a given molecule the distribution of the centre of mass of the remaining molecules may be taken to be spherical symmetric.

The distribution of the molecular long axis about the director is given by an orientational distribution function f(cosθ). As the molecules have no head to tail asymmetry, f (cosθ) is an even function of cosθ. The general expression for the orientational distribution function can be written as [9]:

$$f(\cos\theta) = \sum_{\text{L-even}} (2L+1)/2 \langle P_L(\cos\theta)\rangle P_L(\cos\theta) \qquad 2.1$$

where $P_L(\cos\theta)$ are the L^{th} even order Legendre polynomials, and

$\langle P_L(\cos\theta)\rangle$ are the statistical average given by :-

$$\langle P_L(\cos\theta)\rangle = \int_0^1 P_L(\cos\theta)\, f(\cos\theta)\, d(\cos\theta) \qquad 2.2$$

$\langle P_L\rangle$ are called the orientational order parameters. The expression for the potential of a single molecule in the generalised mean field approximation can be written as

$$V(\cos\theta) = \sum_{\text{L-even}} U_L \langle P_L\rangle P_L(\cos\theta) \qquad 2.3$$

where U_L are the functions of distance between the central molecule and its neighbours only.

Putting $L = 2$ in equation 2.2 we have :

$$\langle P_2(\cos\theta)\rangle = \int_0^1 P_2(\cos\theta)\, f(\cos\theta)\, d(\cos\theta) \qquad 2.4$$

$\langle P_2 \rangle$ is generally called the order parameter. $\langle P_2 \rangle = 0$ for isotropic liquid and $\langle P_2 \rangle = 1$ for perfectly ordered sample.

Equation 2.3 can be written in the expanded form as :

$$V(\cos\theta) = U_2 \langle P_2 \rangle P_2(\cos\theta) + U_4 \langle P_4 \rangle P_4(\cos\theta) + U_6 \langle P_6 \rangle P_6 \cos\theta) + \ldots\ldots \qquad 2.5$$

In the mean field theory of Maier and Saupe, only the first term of the equation 2.5 is retained, so that the expression for the potential energy of a single molecule can be written as :

$$V(\cos\theta) = -v\, P_2(\cos\theta)\, \langle P_2 \rangle \qquad 2.6$$

where $v = -U_2$

The orientational distribution function corresponding to the single molecule is given by :

$$f(\cos\theta) = Z^{-1} \exp[-V(\cos\theta)/kT] \qquad 2.7$$

where Z is the single molecule partition function given by :

$$Z = \int_0^1 \exp[-V(\cos\theta)/kT]\, d(\cos\theta) \qquad 2.8$$

and k is the Boltzmann's constant.

Substituting the value of $f(\cos\theta)$ and $V(\cos\theta)$ from equation 2.7 and equation 2.6 into equation 2.4 we have :

$$\langle P_2(\cos\theta) \rangle = \frac{\int_0^1 P_2(\cos\theta) \exp[P_2(\cos\theta) \langle P_2 \rangle / T^*]\, d(\cos\theta)}{\int_0^1 \exp[P_2(\cos\theta) \langle P_2 \rangle / T^*]\, d(\cos\theta)} \qquad 2.9$$

where $T^* = k T / v$

equation 2.9 is a self consistent equation. For every temperature T^* we can obtain the value of $\langle P_2 \rangle$ that satisfies the self consistence equation. $\langle P_2 \rangle = 0$ is a solution at all temperatures that corresponds to normal isotropic liquid. when $T^* < 0.22284$, two other solutions of $\langle P_2 \rangle$ appear and the state that has minimum free energy will be stable. It has been found that the nematic phase with $\langle P_2 \rangle > 0$ is stable when the T^* satisfies the condition $0 \leq T^* \leq 0.22019$. When $T^* > 0.22019$, the isotropic phase with $\langle P_2 \rangle = 0$ is stable.

The order parameter $\langle P_2 \rangle$ decreases from unity to a minimum value of 0.4289 at $T^*=0.22019$. The nematic isotropic transition takes place at $T^*=0.22019$ and it is a first order phase transition as the order parameter discontinuously changes from $\langle P_2 \rangle = 0.4289$ to $\langle P_2 \rangle = 0$. Although approximation are involved in Maier-Saupe theory, for a number of nematic liquid crystals, the experimental values of $\langle P_2 \rangle$ agree quite well with those predicted by the theory.

2.2 McMillan's theory for smectic phase:

McMillan proposed a simple and elegant description of smectic A by extending the Maier-Saupe theory to include an additional order parameter for characterising the one dimensional translational periodicity of a layered structure. In smectic A phase, there is a periodic density variation along the layer normal (z-direction) in addition to the orientational distribution of the molecular axes. Therefore, the normalised distribution function can be written as:

$$f(\cos\theta) = \sum_{L,\,\text{even}} \sum_{n} A_{L,n}\, P_L(\cos\theta)\, \cos(2\pi n z / d) \qquad 2.10$$

where d is the layer thickness.

The normalising condition for the distribution function is given by:

$$\int_{-1}^{1} \int_{0}^{d} f(\cos\theta, z)\, dz\, d(\cos\theta) = 1 \qquad 2.11$$

McMillan [7,8] following Kobayashi [10,11] expressed the pair potential as:

$$V_M(\cos\theta, z) = -V [\, \delta\alpha\tau \cos(2\pi z / d) + \{\eta + \alpha\delta \cos(2\pi z / d)\} P_2(\cos\theta)] \qquad 2.12$$

where α and δ are the two parameters of the potential. α increases with increasing length of the molecules and δ is the ratio of the translational part of the potential to the orientational part of it. $\eta = \langle P_2(\cos\theta)\rangle$, $\tau = \langle\cos(2\pi z/d)\rangle$ and $\sigma = \langle P_2(\cos\theta)\cos(2\pi z/d)\rangle$ are the orientational, translational and mixed order parameters respectively, and $\langle\ \rangle$ denotes the statistical average of the quantities inside.

The single particle distribution function can be written as:

$$f_M(\cos\theta, z) = Z^{-1} \exp[-V_M(\cos\theta, z) / kT] \qquad 2.13$$

where Z is the partition function given by:

$$Z = \int_{0}^{1} \int_{0}^{d} \exp[-V_M(\cos\theta, z) / kT]\, d(\cos\theta)\, dz \qquad 2.14$$

Once again, three self consistent equations containing η, τ and σ can be written and solved iteratively.

Out of several possible solutions, the thermodynamically stable solution is selected by the criterion of lowest free energy. Depending on the values of the coupling parameters, the following three type of solution are possible:

a/ $\eta = 0, \tau = 0, \sigma = 0$, this solution describes the isotropic liquid phase;

b/ $\eta \neq 0, \tau = 0, \sigma = 0$, this solution describes the nematic phase in accordance with the Maier Saupe theory;

c/ $\eta \neq 0, \tau \neq 0, \sigma \neq 0$, this solution describes the smectic A phase.

For $\alpha > 0.98$, the smectic A phase transforms directly into the isotropic phase, while for $\alpha < 0.98$ there is a smectic A-nematic transition followed by a nematic-isotropic transition at higher temperature. Although nematic-isotropic transition temperature is always first order according to McMillan theory, the smectic A-nematic transition can be either first order or second order. For $T_{AN} / T_{NI} < 0.87$, the smectic A - nematic transition is second order while for $T_{AN} / T_{NI} > 0.87$, the smectic A - nematic transition is first order. T_{AN} and T_{NI} are the smectic A - nematic and nematic - isotropic transition temperature respectively.

2.4 X - ray diffraction from mesophases:

The structure and hence the properties of the liquid crystalline compound can best be understood from the x-ray diffraction studies of the liquid crystal compounds. Although a number of review articles are available in this field, Vainshtein [14] and Leadbetter [17] have given the theoretical interpretation. From x-ray experiment, the Fourier image of the

correlation density function can be determined, the reconstruction of which from the scattered data yields information both on the mutual arrangement of molecules in a liquid crystal and the specific features of the orientational and translational order.

X-ray diffraction of the unoriented nematic phase consists of a uniform halo just like that of an isotropic liquid. The reason behind this is that a nematic liquid crystal generally consists of a large number of domains, the molecules being ordered within each domain along the director **n**, but there is no preferred direction for the sample as a whole so that the diffraction pattern has a symmetry of revolution around the direction of the x-ray beam. However, application of suitable magnetic or electric field can produce a 'monodomain' or 'aligned' or 'oriented' sample of liquid crystal.

The small angle x-ray diffraction pattern from a nematic liquid crystal oriented perpendicular to the direction of the incident x-ray beam is shown in the Figure 2.1a. In the diffraction pattern, the main halo splits into two crescents for each of which intensity is maximum in the equatorial direction, i.e. perpendicular to the director. These crescents are formed mainly due to the intermolecular scattering and the corresponding Bragg angle is a measure of lateral intermolecular distance. The angular distribution of the x-ray intensity (Fig. 2.1a), I (ψ) vs. ψ curve, also gives the orientational distribution function f($\cos\theta$) and order parameter $\langle P_L \rangle$, (L= 2, 4).

In the meridional direction, parallel to the director, two crescents are also observed at much smaller angle and the corresponding Bragg angle is a measure of apparent molecular length. Sometimes, the inner diffuse crescents are replaced by sharp spots and the corresponding

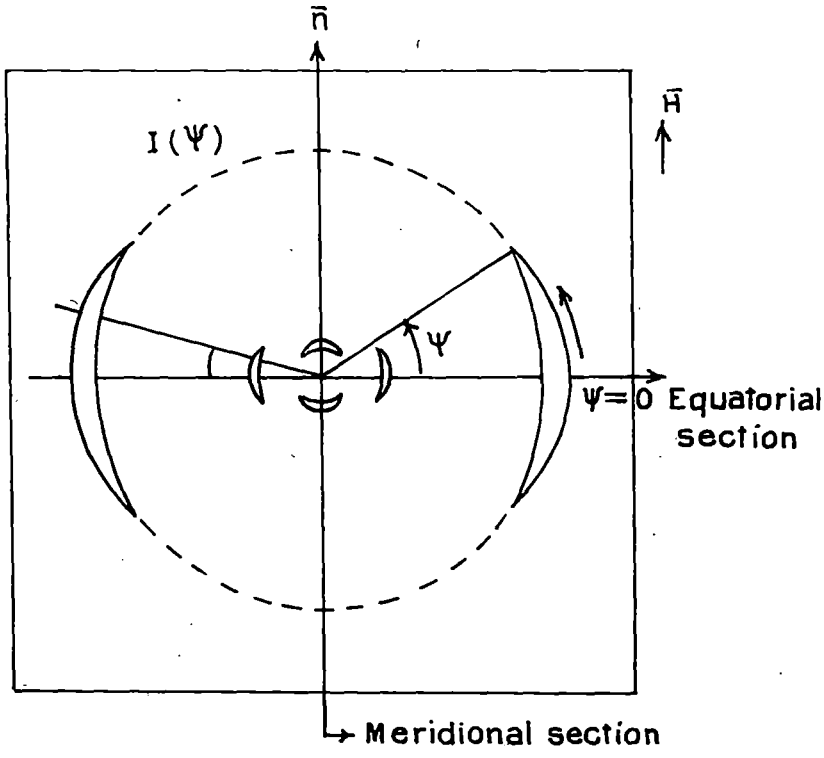

Figure 2.1a. Schematic representation of the x-ray diffraction pattern of an oriented nematic liquid crystal.

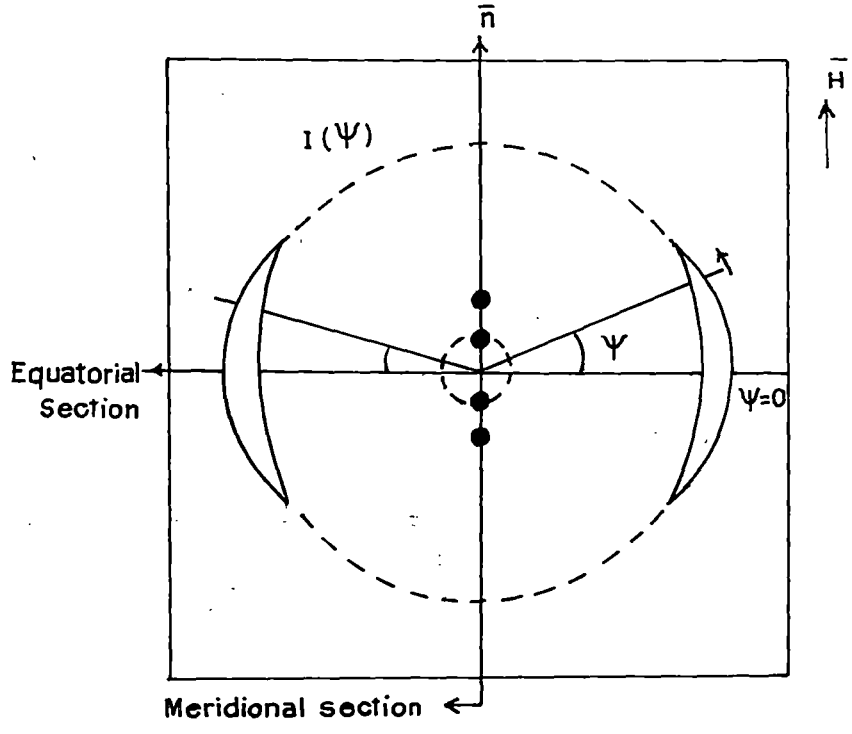

Figure 2.1b. Schematic representation of the x-ray diffraction pattern of an oriented smectic A liquid crystal.

phase is called "cybotactic phase". The presence of the sharp spots indicates smectic like clusters in the nematic phase which are called "cybotactic" groups [20].

The x-ray diffraction pattern of smectic A phase is shown in Figure 2.1b. The meridional spots are formed due to Bragg reflection from the layers and provide the value of layer thickness. Since smectic A can have only quasi-long range order along its layer normal [3,21], the second order Bragg reflections in the meridional direction are generally very weak and are often absent in the x-ray photographs. When present, these second order reflections provide a method for calculating τ, the translational order parameter.

In our x-ray photographs of the liquid crystals, sometimes other faint diffuse spots are also present, which may be due to (a) intra-molecular atomic scattering (b) next nearest neighbour intermolecular scattering and (c) effect of white radiation contained in Ni filtered Cu-radiation. However, we do not consider such diffraction patterns in our analysis.

2.5 Experimental technique and data analysis; X-ray diffraction studies:

The x-ray diffraction set up has been designed and fabricated in our laboratory by Jha and Paul [22]. The schemetic representation of the whole set up is shown in Figure 2.2. The brief description of the set up is as follows:

The x-ray generator is that of Radon house (India) and the x-ray tube with copper - target is used. The set up has flat-plate camera provided with the

sample holder (8) having heating arrangement. The sample holder is fitted with a changeable collimator (2) and is well insulated from the surroundings by asbestos cement. The sample holder is supported by four brass posts (16) that are rigidly attached to the heavy brass plate (12). The brass plate is also fitted with the film cassette holder (11) and the space between the film cassette and the sample holder are separated by adjustable spacer (15). The sample was taken in a thin walled lithium glass capillary of diameter 1mm and is introduced into the sample holder. The camera is then placed between the pole pieces of an electromagnet in such a way that the sample remains at the centre of the pole pieces (17). The magnetic field acts along the axis of the capillary and the pole pieces can be brought very close to each other to provide strong magnetic field of about 5 Kilogauss. The strength of the magnetic field was measured by sensitive Gaussmeter (ECIL model GH 867). For better collimation of the x-ray beam, levelling screws (13) are provided on the brass plate. At first the sample was heated to the isotropic phase and was slowly cooled to the desired temperature in presence of the magnetic field. The temperature of the sample holder and hence the sample was maintained constant within ± 0.5 °C by a temperature controller (Indotherm model IT401D2). The film cassette is loaded with new film and is then placed on the cassette holder. The film is then exposed to x-ray diffracted from the sample, the direct beam being stopped by a beam stop. The magnetic field was kept on during the exposure of the film. The exposure time in our experiment was about three hours. Also, all the x-ray photographs were taken by using Ni-filter of thickness 0.009 mm which gives mainly the monochromatic Cu K_α radiation of wavelength 1.5418 Å. Furthermore, the incoming x-ray beam was collimated by a collimator of aperture 0.8 mm. X-ray photographs were taken for the same

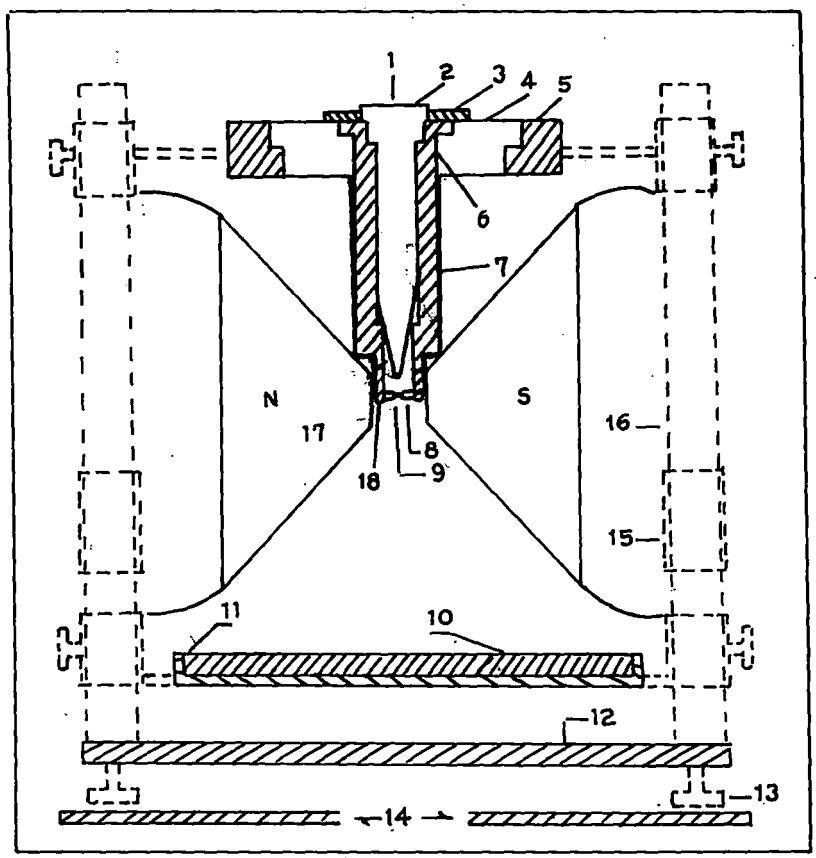

Figure 2.2 Sectional diagram of the X-ray diffraction camera.

1. X-ray 2. Collimator 3. Brass ring 4. Ring of syndanyo board 5. Brass ring 6. Cylindrical brass chamber 7. Asbestos insulation and heater winding 8. Specimen holder and thermocouple 9. Sample 10. Film Cassette 11. Film cassette holder 12. Base plate 13. Levelling screw 14. Brass plates over the coils of the electromagnet 15. Removable spacer 16. Supporting brass stand 17. Pole peices 18. Asbestos insulation.

sample at various temperatures. In my experiment, the sample to film distance was varied from 8 cm to 10 cm depending upon the sample.

The spacer gives only apparent distance between the sample and the film. To get the exact sample to film distance, I have taken aluminium powder photograph. The Bragg angle corresponding to the hkl reflecting plane for the aluminium (F.C.C structure) can be determined from the equation [23]:

$$\sin\theta' = \lambda (h^2 + k^2 + l^2)^{1/2} / 2a \qquad 2.15$$

Thus measuring the diameter of the diffraction rings corresponding to (111) and (200) reflections [22] and the values of Bragg angle from equation 2.15, the actual distance between the sample and the film can be obtained from the relation :

$$\tan (2\theta') = \text{Radius of the ring / Sample to film distance} \qquad 2.14$$

The correction term was calculated and the apparent distance given by spacer was corrected to get the exact value of sample to film distance.

a/ Conversion of optical density to x-ray intensity:

The optical density of the x-ray photographs were measured by a Carl Zeiss Microdensitometer (MD100) which has potentiometric recording (k200) facility for linear scanning. The optical density values obtained from the densitometric scan were then converted to relative intensity values by a method explained by Klug and Alexander [24]. A strip of film was kept inside a film holder provided with a rectangular

opening on a lead sheet and was kept at a fixed distance from the x-ray tube. Multiple film technique was used to prepare an intensity scale by exposing different portion of the film to x-rays coming through the rectangular opening with different exposure times (5sec, 10sec, 20sec,...etc.). The optical densities of these spots were measured with the help of microdensitometer. Since the microdensitometer zeroing was adjusted on unexposed x-ray film, we need not subtract the optical density of unexposed film from the measured data. A graph is then plotted with optical density vs. time in seconds. Since x-ray intensity is proportional to the time of exposure, the optical density vs. time in second curve actually corresponds to x-ray intensity and hence it is used as calibration curve to convert x-ray intensity to optical density.

b/ Circular scanning of x-ray photographs:

To perform circular scanning of the x-ray film, densitometer is provided with the rotating stage, fabricated in our laboratory, to facilitate 360°-scanning of the photographs. Photographs were scanned to measure angular intensity distribution $I(\psi)$ which was used to calculate the orientational distribution function $f(\beta)$ and order parameters $< P_2 >$ and $< P_4 >$. Reading of the circular scan of the outer diffraction arc were taken from $\psi = 0$ to $\psi = 360°$ at 1° interval near the peak and at larger intervals elsewhere. The optical density values, thus obtained, were converted into corresponding x-ray intensity with the help of the calibration curve. The experimental intensities values were then corrected for the background intensity values arising due to the air scattering. The peak intensity position which corresponds to $\psi = 0$ was determined from intensity $I(\psi)$ vs. angle (ψ) curve. $I(\psi)$ vs. ψ curve were smoothed, and nineteen values of $I(\psi)$

were taken from $\psi = 0$ to $\psi = 90^{\circ}$ at 5° intervals. From the values of $I(\psi)$, we have calculated the distribution function $f(\beta)$, and order parameters ($\langle P_2 \rangle$ and $\langle P_4 \rangle$) by Lead better's expression. A computer program was written in our laboratory for these calculations.

c/ Linear Scanning of x-ray photographs:

The linear scan of the x-ray photographs were performed by using the potentiometric recorder and the recorder plotted a graph of optical density vs. linear distance. The distance between the peak position gives the diameter of the diffraction ring.

2.6 Orientational distribution functions and order parameters:

As it has been mentioned in Chapter-1, the liquid crystals are composed of rod like molecules which are cylindircally symmetric about their long axes. Both the nematic and smectic A phases have uniaxial symmetry which is parallel to the unit vector **n** called the director. The orientational distribution function describes how the moleculer long axes are distributed about the director; it gives the probability of finding a molecule at some prescribed angle β from **n**. The x-ray diffraction pattern of an oriented sample consists of equatorial arcs. The orientational distribution function is related to the distribution of x-ray intensity along the diffused equatorial axes according to the following equation [17]:

$$I(\psi) = c \int_{\beta=\psi}^{\pi/2} f_d(\beta) \sec^2 \psi \, [\tan^2 \beta - \tan^2 \psi]^{-1/2} \sin \beta \, d\beta \qquad 2.16$$

where $f_d(\beta)$ describes the distribution function of the directors of clusters in which the molecules are perfectly aligned. The equation 2.16 can be numerically inverted to give $f_d(\beta)$ which are assumed to be close to the singlet distribution function $f(\beta)$.

The orientational order parameter $\langle P_2 \rangle$ and $\langle P_4 \rangle$ were calculated by using the following equation :

$$\langle P_L \rangle = \int_0^1 P_L(\cos\beta)\, f_d(\beta)\, d(\cos\beta) \Big/ \int_0^1 f_d(\beta)\, d(\cos\beta) \qquad 2.17$$

where, $L = 2,4$.

The method of obtaining intensity values $I(\psi)$ from the measured optical densities of the x-ray diffraction photographs has been described in section 2.5b. To calculate $f_d(\beta)$ and order parameter we need $I(\psi)$ values from $\psi = 0$ to $\psi = 90^0$ i.e. one quadrant. I have measured $I(\psi)$ values of four quadrants separately and the average values of $I(\psi)$ is considered to calculate $f(\beta)$ as well as $\langle P_2 \rangle$ and $\langle P_4 \rangle$ for all the samples. The errors in the calculation of $\langle P_2 \rangle$ and $\langle P_4 \rangle$ in our experiment are estimated to be within $\pm$ 0.02.

2.7 Molecular parameters from x-rays studies:

a/ Intermolecular distance:

The average lateral distance between the neighbouring molecules (D) is related to the corresponding Bragg angle (2θ) according to the formula [20];

$$2\, D \sin\theta = k\, \lambda \qquad 2.18$$

where, 2θ is the Bragg angle for the equatorial diffraction, λ is the wave length of the x-ray and k is a constant which comes from the cylindrical symmetry of the system. Recent calculation [30] have shown that the value of k depends on the order parameter of the sample under consideration. For perfectly ordered state k = 1.117 as given by de Vries [20]. Since the variation of k with $< P_2 >$ is small, I have used the value k = 1.117 for all the calculations.

b/ Apparent molecular length or layer thickness:

To calculate the apparent molecular length (or layer thickness) (d), I have used the Bragg equation ($2\ d \sin\theta = \lambda$), where θ is the Bragg angle for the meridional diffraction crescent (or spots) for an aligned sample or for the inner halo (or ring)in the case of unaligned sample.

2.8 Refractive index of mesophases:

Most of the nematic liquid crystals are optically uniaxial and strongly birefringent. A uniaxial liquid crystal has two principal refractive indices viz. ordinary refractive index (n_0) and extraordinary refractive index (n_e). The birefringence is defined by the following equation:

$$\Delta n = n_e - n_o \qquad 2.19$$

The first birefringence measurement were made by E. Dorn [31] and its theoretical explanation was given by O.Weiner [33] and H.Zocher [34,35]. Birefringence is positive for conventional nematics with its value lying between 0 to 0.4, while it is negative for chiral nematics. Refractive indices of the smectic phases have also been measured [43-45]. To evaluate the molecular polarisabilities of the liquid crystal it is necessary to consider the anisotropic internal field that arises due to anisotropic

molecular arrangements in the liquid crystals. Hence, in case of liquid crystals the well known Lorentz-Lorentz formula for isotropic media is replaced by Neugebauer formula [46] or Vuks formula [47]. Saupe and Maier [48] also applied a more elaborate internal field suggested by Neugebauer.

I have measured the ordinary and extra ordinary refractive index of the nematic liquid crystals, smectics as well that of the re-entrant nematic phase and then calculated the effective polarisabilities α_0 and α_e of the anisotropic liquid crystals by using the two different internal field models [46,47]. Finally orientational order parameter $\langle P_2 \rangle$ was calculated.

a/ Neugebauer Method:

Neugebauer [46] extended Lorentz-Lorentz equations for an isotropic system to an anisotropic system. In this model the effective polarisabilities α_0 and α_e of the liquid crystals are related to the refractive indices n_e and n_0 according to the following equations:

$$n_e^2 - 1 = 4\pi N \alpha_e (1 - N \alpha_e \gamma_e)^{-1} \qquad 2.20$$

and $$n_0^2 - 1 = 4\pi N \alpha_0 (1 - N \alpha_0 \gamma_0)^{-1} \qquad 2.21$$

where, γ_o and γ_e are the respective internal field constants for ordinary and extraordinary rays, N is the number of molecules per c.c. and n_e and n_0 are the extraordinary and ordinary refractive indices respectively. The relevant equations for calculating polarisabilities (α_0, α_e) as obtained from the equations 2.20 and 2.21 are as follows:

$$1/\alpha_e + 2/\alpha_o = [4\pi N/3] [\{ (n_e^2 + 2) / (n_e^2 - 1)\} + \{2 (n_o^2 + 2) / (n_o^2 - 1) \}] \qquad 2.22$$

and

$$\alpha_e + 2\,\alpha_o = [9/4\pi N]\,[(n^2 - 1)/(n^2 + 2)] \qquad 2.23$$

where,

$n^2 = (2n_o^2 + n_e^2)/3$, n is the mean refractive index.

α_o and α_e values are obtained by directly solving equations 2.22 and 2.23.

b/ Vuks method:

Vuks has derived another formula for polarisabilities associated with anisotropic molecules by assuming that the internal field is independent of orientation. The Vuks formula relating the molecular polarisabilities (α_o, α_e) and refractive indices (n_o, n_e) are as follows :

$$(n_o^2 - 1)/(n^2 + 2) = 4\pi N\alpha_o/3 \qquad 2.24$$

and

$$(n_e^2 - 1)/(n^2 + 2) = 4\pi N\alpha_e/3 \qquad 2.25$$

where,

$n^2 = (2n_o^2 + n_e^2)/3$, n is the mean refractive index.

α_o and α_e can be calculated directly from the refractive index values.

2.9 Calculation of order parameter from the polarisabilities:

The relation between orientational order parameter $\langle P_2 \rangle$ and the principal polarisabilities are given by de Gennes [49] as :

$$\alpha_e = \bar{\alpha} + (2/3)\,\alpha_a \langle P_2 \rangle \qquad 2.26$$

$$\alpha_o = \bar{\alpha} - (1/3)\,\alpha_a \langle P_2 \rangle \qquad 2.27$$

where,

$\bar{\alpha} = (2\alpha_o + \alpha_e)/3$ is the mean polarisability

and

$\alpha_a = (\alpha_\parallel - \alpha_\perp)$ is the molecular polarisability anisotropy where $\alpha_\parallel$ and $\alpha_\perp$ are the principal polarisabilities, parallel and perpendicular to the long axes of the molecules in the crystalline state. Due to strong absorption in the solid phase, we could not measure α_a directly. to get the value of α_a, Haller's extrapolation method [50] was adopted. The graph was plotted with $\log(\alpha_e-\alpha_o)$ vs. $\log(T_c-T)$ giving a straight line which is extrapolated to $\log(T_c)$ where T_c corresponds to nematic isotropic transition temperature. the limiting value of $(\alpha_e-\alpha_o)$ at $T = 0\ ^oK$ is assumed to correspond to $(\alpha_\parallel-\alpha_\perp)$.

From equation 2.26 and 2.27 we have

$$\langle P_2 \rangle = \frac{\alpha_e - \alpha_o}{\alpha_\parallel - \alpha_\perp} \qquad 2.28$$

For a given sample, α_e and α_o are calculated at various constant temperatures from which $(\alpha_\parallel-\alpha_\perp)$ is obtained. The order parameter $\langle P_2 \rangle$ is then calculated by using equation 2.28.

2.10 Measurement of refractive indices :

Refractive indices (n_o, n_e) of a liquid crystal for ordinary and extra-ordinary rays were measured by using thin hallow prisms with the refracting angle less than 2^o. The details of the preparation of the prism and the experimental procedure have already been reported by Zemindar et al [51]. To prepare prism optically flat glass plates are taken, and they are first cleaned by conc. HNO_3 and then by acetone. One surface of the glass plates was rubbed on bond paper in a direction parallel to one of their

edges. The rubbed surface is then coated with thin layer of 1 % solution of polyvinyl alcohol and then dried. The preferred direction on the substrate can be obtained by rubbing the same surface in the same direction again by a tissue paper. The prism was then prepared by placing the rubbed surfaces inside, with the rubbing direction parallel to the refracting edge of the prism. A thin glass spacer was introduced between one of the vertical edge of the prism for getting the desired refracting angle of the prism. The glass plate of the prism were sealed together by using high temperature adhesive and were baked in an oven. Liquid crystal sample was introduced into the prism from its top open side by melting. The system was alternately heated to isotropic phase and cooled slowly so that the liquid crystals were perfectly aligned with its optic axis parallel to the refraction edge of the prism. The prism was then placed inside a brass oven provided with transparent opening at the centre and the temperature of the oven was maintained constant at a desired value by a temperature controller (Indotherm model IT401D2) within an accuracy of ±0.5 °C. The refractive indices (n_o, n_e) were measured for four different wavelengths (λ = 6907Å, 5890Å, 5461Å, 4358 Å), corresponding to mercury source by means of a precision spectrometer and an optical monochromator.

2.11 Measurements of densities:

The densities of the liquid crystals were measured with the help of a dilatometer of the capillary type. A weighed amount of the liquid crystal was introduced inside the dilatometer which was kept immersed in a thermostated liquid bath. The height of the liquid crystal column was measured at different temperatures with the help of a travelling microscope. But before taking the reading, sufficient time was given to

attain equilibrium at any desired temperature. The densities were then calculated by making corrections for the expansion of glass capillary. The accuracy of density measurement lies within ± 0.1 %.

2.12 Magnetic susceptibility measurements:

Introduction:

The determination of diamagnetic properties is of great importance in the study of liquid crystals. All anisotropic properties of liquid crystals are related to the orientational order parameter $\langle P_2 \rangle$ in a more or less complicated way. Since the molecular susceptibility of a liquid crystal is anisotropic the orientational order parameter is related to the magnetic susceptibility [52-55] in a more or less straight forward way. It is considered to be one of the best methods for studying the variation of order parameter with temperature despite the experimental difficulties in measuring the susceptibility. The theoretical treatment regarding the effect of external magnetic field on liquid crystal was given by J.P.Dias [56] and the magnetic alignment of the liquid crystal was explained by J.O.Kessler [57]

To investigate the effect of external magnetic field on liquid crystal materials we first define the magnetisation **M** induced by the applied magnetic field **H** according to the following equation:

$$M_\alpha = \chi_{\alpha\beta} H_\beta \qquad 2.29$$

$$\alpha,\beta = x, y, z$$

where $\chi_{\alpha\beta}$ is an element of the magnetic susceptibility tensor $\bar{\chi}$ and the summation convention over repeated index is followed.

For uniaxial phase like nematic or smectic A phase and choosing the director along the **n** along the z-axis we have:

$$\bar{\chi} = \begin{bmatrix} \chi_\perp & 0 & 0 \\ 0 & \chi_\perp & 0 \\ 0 & 0 & \chi_\parallel \end{bmatrix}$$

The subscript $\parallel$ and $\perp$ indicates the component parallel and perpendicular to the director respectively. The average susceptibility is given by

$$\bar{\chi} = (1/3) \sum_{\gamma} \chi_{\gamma\gamma}$$

$$= (1/3)(\chi_\parallel + 2\chi_\perp) \qquad 2.30$$

The magnetic susceptibility anisotropy is defined as :

$$\Delta\chi = \chi_\parallel - \chi_\perp$$

$$= (3/2)(\chi_\parallel - \bar{\chi}) \qquad 2.31$$

Hence the susceptibility tensor has only two different non zero elements, and we find :

$$\mathbf{M} = \chi_\parallel \mathbf{H}, \text{ if } \mathbf{H} \parallel \mathbf{n}$$

$$\mathbf{M} = \chi_\perp \mathbf{H}, \text{ if } \mathbf{H} \perp \mathbf{n}$$

For an arbitrary angle (θ) between **H** and **n** we derive for total magnetisation

$$\mathbf{M} = \chi_\perp \mathbf{H} + \Delta\chi (\mathbf{H}.\ \mathbf{n})\mathbf{n} \qquad 2.32$$

Therefore the free energy in a magnetic field is given by:

$$F_{magn} = -\int_0^H \mathbf{M}.\, d\mathbf{H}$$

$$= -(1/2)\chi_\perp H^2 - (1/2)\Delta\chi\ (\mathbf{H}.\mathbf{n})^2$$

2.33

Since the first term of the above equation is free from **n**, it may be omitted as far as orientation related problems are concerned. For positive anisotropy i.e. $\Delta\chi > 0$, the last term is minimised when **H** is collinear with **n**. Therefore the liquid crystal with positive $\Delta\chi$ tend to align with their molecular long axes along the direction of the applied magnetic field. However, for liquid crystal with negative $\Delta\chi$, the molecules tend to align perpendicular to the applied magnetic field. Hence the coupling to the director occurs through the anisotropy of the molecular susceptibility.

2.13 Relation between order parameter and magnetic anisotropy:

The order parameter **Q** is defined by considering the anisotropic part of the susceptibility χ as follows :

$$Q_{\alpha\beta} = \chi_{\alpha\beta} - \delta_{\alpha\beta}\ \bar{\chi} \qquad 2.34$$

where, $\alpha, \beta = x, y, z$ and $\delta_{\alpha\beta}$ is the kronecker delta function, **Q** is a second rank tensor, which is diagonal.

If we choose the director **n** along the z-axis, then **Q** has zero trace and vanishes for the isotropic phase. If we consider uniaxial symmetry around **n**, it is sufficient to consider only one element Q_{zz} of **Q**.

Equation 2.34 can also be written in the form:

$$Q_{\alpha\beta} = \chi_{\alpha\beta} - (1/3)\delta_{\alpha\beta} \sum_{\gamma} \chi_{\gamma\gamma} \qquad 2.35$$

Therefore,

$$Q_{zz} = \chi_{zz} - (1/3)\{\chi_{xx} + \chi_{yy} + \chi_{zz}\}$$
$$= (2/3)(\chi_{\parallel} - \chi_{\perp}) \qquad 2.36$$

Here we assume

$$\chi_{xx} = \chi_{yy} = \chi_{\perp} \text{ and } \chi_{zz} = \chi_{\parallel}$$

In order to relate **Q** to the microscopic order parameter S, let **K** be the tensor of the molecular magnetic polarisability which is assumed to be diagonal in the molecule - fixed co-ordinate system ξ,η,ζ.

Therefore,

$$\chi_{\alpha\beta} = N \sum_{i,j} K_{ij} \langle i_\alpha j_\beta \rangle \qquad 2.37$$

where $i, j = \xi,\eta,\zeta$.

$\alpha, \beta = x, y, z$.

i_α is the α - component of a unit vector along ξ,η,ζ axes, N is the number of molecules per unit volume and the bracket $\langle\ \rangle$ stands for statistical average.

Using equation 2.37, the order parameter represented by equation 2.35 can be expressed as :

$$Q_{\alpha\beta} = N \sum_{i,j} K_{ij} \langle i_\alpha j_\beta - (1/3)\ \delta_{\alpha\beta}\delta_{ij} \rangle \qquad 2.38$$

Therefore,

$$\begin{aligned} Q_{zz} &= N \sum_{i,j} K_{ij} \langle i_z j_z - (1/3)\ \delta_{ij} \rangle \\ &= (2/3) N \sum_{i,j} K_{ij}\ (1/2) \langle 3\, i_z j_z - \delta_{ij} \rangle \\ &= (2/3) N \sum_{i,j} K_{ij}\ S_{i,j} \end{aligned} \qquad 2.39$$

where,

$S_{i,j} = (1/2) \langle 3\, i_z j_z - \delta_{ij} \rangle$ is the generalised order parameter.

From equation 2.36 and 2.39 we have:

$$\begin{aligned} Q_{zz} &= (2/3)(\chi_{\parallel} - \chi_{\perp}) \\ &= (2/3) N \sum_{i,j} K_{ij}\ S_{i,j} \end{aligned} \qquad 2.40$$

As S_{ij} is diagonal in a molecular fixed co-ordinate system ξ, η, ζ with the ζ-axis as the long molecular axis and has zero trace, there are two independent scalar order parameter, for which we choose $S = S_{\zeta\zeta}$ and $D = S_{\eta\eta} - S_{\zeta\zeta}$.

Thus equation 2.40 can be written as :

$$(\chi_{\parallel} - \chi_{\perp}) / N = \{K_{\zeta\zeta} - (1/2)(K_{\eta\eta} + K_{\zeta\zeta})\} S + (1/2)(K_{\zeta\zeta} - K_{\eta\eta}) D \qquad 2.41$$

where S is the order parameter which have a value between 0 and 1.

Therefore,

$$S = 1/2 < 3\zeta_z^2 - 1 >$$
$$= 1/2 < 3\cos^2\theta - 1 >$$

where 'θ' is the angle between z and ζ axes.

Furthermore,

$$D = (1/2) < 3\xi_z^2 - 1 > - (1/2) < 3\eta_z^2 - 1 >$$
$$= (3/2) < \xi_z^2 - \eta_z^2 >$$
$$= (3/2) < \sin^2\theta \cos 2\psi >$$

where ψ is the Euler angle specifying the rotation around the ζ-axis. D measures the difference in tendency of the two transverse molecular axes to project on the z-axis. By considering the molecule to be axially symmetric, we have D = 0.

Now equation 2.41 can be written as :

$$(\chi_{\parallel} - \chi_{\perp}) = (\chi_l - \chi_t) S \qquad 2.42$$

where $\chi_l = N K_{\zeta\zeta}$ and $\chi_t = (1/2) N (K_{\eta\eta} + K_{\zeta\zeta})$

Equation 9.42 is known as Tsvetkov's expression for order parameters [44,45]. To determine the order parameter (S) we need the value of

(χ_l - χ_t) which can be obtained from solid single crystal measurements. An alternative method to estimate(χ_l - χ_t) is against temperature due to Haller et al [50] A logarithmic plot of (χ_l - χ_t) against ln(T_c-T) often gives straight line, and (χ_l - χ_t) is obtained by extrapolating to T = 0 and assuming S = 1 at that point. I have adopted Haller's method to estimate the value of order parameter.

2.14 Determination of $\Delta\chi$:

The magnetic susceptibility have been measured by the classical Faraday-Curie method. The total force (F) experienced by a sample in an inhomogeneous magnetic field with a gradient in the horizontal x-direction is given by:

$$F = (1/2)\,(m\chi - m_o\,\chi_o)\,(dH^2/dx)_{av} \qquad 2.43$$

where χ, m are the mass susceptibility and the mass of the sample and χ_o, m_o are those of air driven out of the sample. The subscript 'av' indicates the average value. If we assume that the sample is replaced by almost same volume of the reference sample and is placed at more or less at the same position between the pole pieces of the magnet, then (dH^2/dx) will be same for both the cases. By indicating the reference sample with the subscript 'r', the force acting on the reference sample is given by:

$$F = (1/2)\,(m_r\chi_r - m_o\,\chi_o)\,(dH^2/dx)_{av} \qquad 2.44$$

From equation 2.43 and 2.44 we can write:

$$\chi(t) = \frac{F}{F_r}\,\frac{m_r}{m}\left[\chi_r - \frac{\rho_o(t_o)}{\rho_r(t_o)}\,\chi_o(t_o)\right] + \frac{\rho_o(t)}{\rho(t)}\,\chi_o(t) \qquad 2.45$$

where ρ, ρ_r and ρ_o are densities of the experimental sample, reference sample and air respectively; t_o is the temperature at which the measurement of the reference sample is made.

The sample was taken in a cylindrical quartz container having a volume of nearly 0.1 cm^3. It was hung by a glass capillary between the pole pieces, the value of (dH^2/dx) being 1.1 K. $gauss^2$ / cm. approximately. The value of (dH^2/dx) is constant within 1% for 1cm. length along x-direction while along y and z direction (dH^2/dx) is practically constant over sufficiently large distances. The temperature of the sample was maintained constant within $\pm 0.5^oC$ by temperature controller (Indotherm model 401 D2). The whole system is evacuated to avoid disturbance to the balance due to convection in air. The accuracy of measurement using this balance is about 1%.

I have used trans-decaline ($\chi_r = 0.779 \times 10^{-6}$ c.g.s.unit) [58] a non-volatile liquid at room temperature as a reference substance. Density of reference sample is 0.869 gm/c.c. [59]. Using the magnetic susceptibility of air ($\chi_o = 106.3 \times 10^{-6}$ c.g.s.unit at 20^oC) [60], the curie law $\chi_o \sim 1/T$, the tabulated density of air [61], the necessary correction as given by equation 2.43 can be calculated. Error due to the influence of dissolved oxygen has been discussed and ignored by de Jeu et al [62]. I have also neglected the influence of dissolved oxygen.

In the experimental arrangement, the force on the sample is exactly balanced by the force exerted on the horizontal coil, rigidly attached to the balance beam, placed inside the hollow permanent magnet with a uniform radial field and carrying a suitable current i. This force due to the field on the coil is given by :

$$F = 2\pi rniH$$

where, n = number of turns in the coil, r = radius of the coil, H = magnetic field intensity.

In general the suspended system will experience a pull even in the absence of any magnetic sample to balance the pull, we must pass an initial current i_o through the coil. In our set up, instead of the current we measured voltage drop across a standard resistance of the order of 10 K. ohms with the help of high precision digital voltmeter. So the final expression for the susceptibility becomes:

$$\chi(t) = \frac{(v - v_o)}{(v_r - v_o)} \frac{m_r}{m} \left[\chi_r - \frac{\rho_o(t_o)}{\rho_r(t_o)} \chi_o(t_o) \right] + \frac{\rho_o(t)}{\rho(t)} \chi_o(t) \qquad 2.46$$

All the values of magnetic susceptibilities given by me in this thesis are mass susceptibility in c.g.s. unit (erg gauss^{-2} gm^{-1}).

2.15 Description of the experimental set-up for determination of diamagnetic anisotropy ($\Delta\chi$):

The electromagnetic balance for measuring susceptibilities have been designed and fabricated in our laboratory by M. Mitra and R. Paul [63]. Basically the instrument is of the Curie type, the movement of the arms being restricted to the horizontal plane. the schematic diagram of the apparatus is shown in Figure 2.3.

It consists of a horizontal light glass beam A, kept suspended at the middle with vertically stretched phosphor-bronze strips. The upper strip B, is soldered to a torsion head T used for adjusting the position of the beam, whereas, the lower one B′ terminates in an elliptic spring E secured to a universal adjustable holder H which can be moved horizontally in two

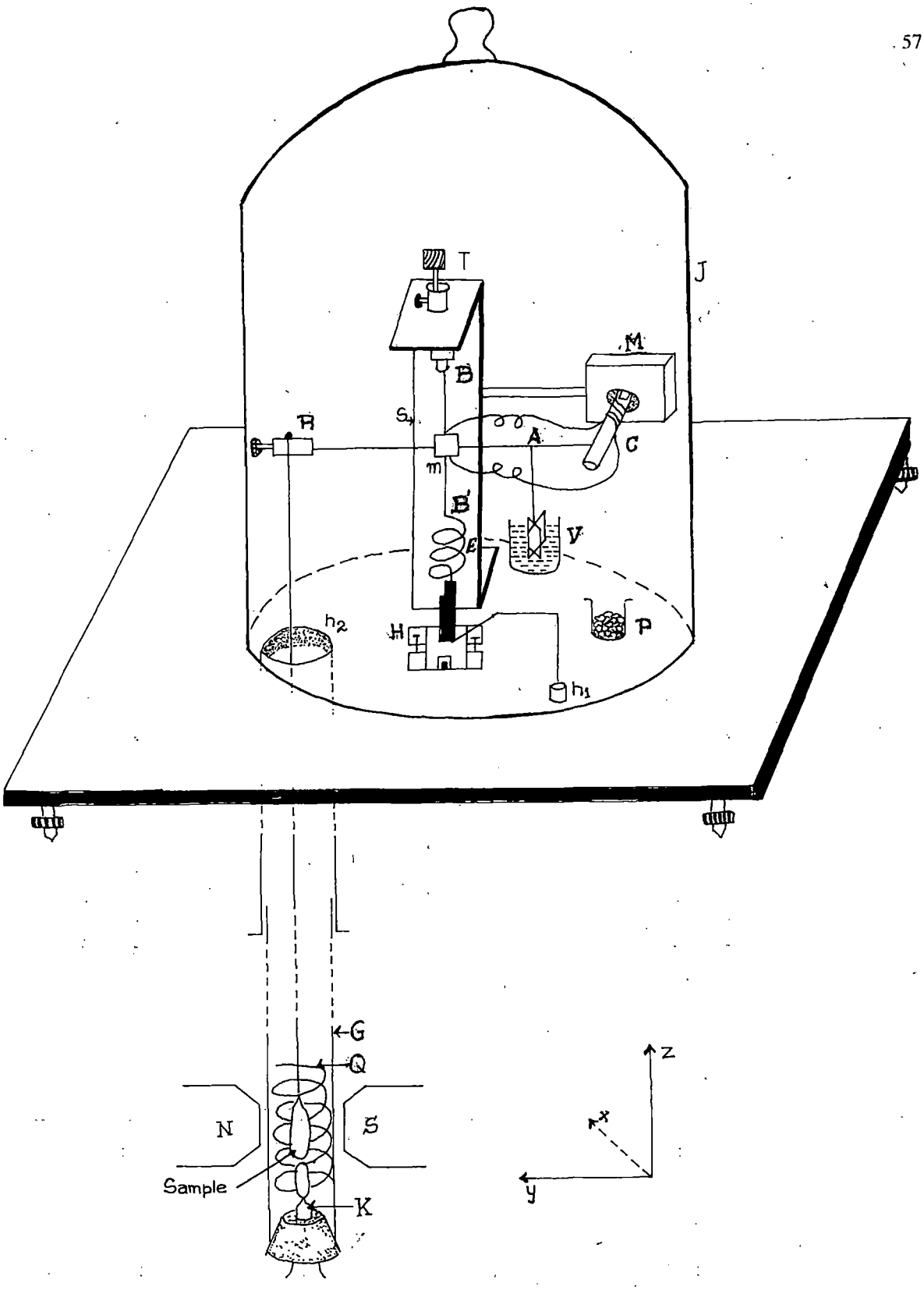

Figure 2.3 Schematic diagram of the apparatus for measuring magnetic susceptibility. T- Torsion head, S- Brass pillar, B, B′ - Phospher-bronze strip, m- mirror, A- Balance beam, M- Magnet, C- Coil, E- Spring, G- Glass tube, Q- Heater, K- Thermo-couple, P- Beaker Containing calcium chloride, V- Vane, H- Adjustable platform, J- Bell-jar, p- Brass plate, R- Perspex block.

directions. The torsion head is fixed to a brass pillar S and the holder H is fixed on a flat brass plate b resting on levelling screws.

A small perspex block R is attached to one end of an arm of the balance beam and has a vertical hole to which is attached a long capillary tube carrying a sample holder. A damping vane V made of thin mica sheet dipping into diffuse pump oil fixed to the other side of the glass beam effectively damps out all spurious vibrations. On the same side of the balance beam is attached a balancing coil of 50 turns of 42 s.w.g. enamelled copper wire wound over a hollow perspex cylinder C and the coil is free to move inside a hollow magnet M having a radial field of about 200 gauss. The phosphor -bronze strips acts as a suspension wire as well as electric connection of the coil. The balance assembly is covered with a greased ground bell jar J. Two holes h_1 and h_2 are drilled in the base plate. In one of this hole, is fixed an ebonite block with binding terminal, sealed vacuum tight with araldite, for leading in the coil currents. The other terminal of the coil is attached to the brass plate. The second aperture h_2 about 3 cm in diameter is fitted with a brass collar for fitting the glass tube extension of the experimental chamber. The joint of the glass tube G and brass tube is made vacuum tight with o-ring. A heater Q of constantant wire and a thermocouple K is fixed through a rubber stopper and is introduced into the glass tube which is made vacuum tight. The sample holder, thermocouple and the heater are placed between the pole pieces of an electromagnet. The brass tube is also provided with a side tube (t) through which the balance chamber and the experimental chamber can be evacuated. The sucksmith form of a pole piece is adopted and any change in the position of the sample was detected with the help of a pair of matched photocells.

It should be notated that since the director of the mesogens aligns itself in the direction of the magnetic field ($\Delta\chi > 0$) in most samples, the magnetic susceptibility determined by this method is $\chi_{\parallel}$ in mesophase and $\bar{\chi}$ in isotropic phase. Since non-metallic organic mesogens are diamagnetic, $\bar{\chi}$ should be independent of temperature. Hence, using equation 2.31 we get $\Delta\chi = 1.5\ (\chi_{\parallel} - \bar{\chi})$, $\Delta\chi$ being the magnetic susceptibility anisptropy. Order parameter is then calculated using equation 2.42.

2.16 Elastic constant and deformation free energy of nematic liquid crystal:

The elastic constants of a liquid crystal are restoring torque which become apparent when the system is perturbed from its equilibrium configuration. In display devices, the electric or the magnetic field induces the initial perturbation and as such the balance between elastic and electric or magnetic forces determines the static deformation pattern of a liquid crystal.

Although various properties of mesophase transitions could be explained in terms of molecular theories but its use to explain the elastic phenomena of the liquid crystal is not obvious as it involves the response of bulk liquid crystal samples to external disturbances. Elastic behaviour of the liquid crystal can be more conveniently explained by regarding liquid crystal as a continuous medium with a set of elastic constants. Based on this viewpoint, Zocher [65], Oseen [66], and Frank [67] developed a phenomenological continuum theory of liquid crystals which can successfully explain the various magnetic or electric field induced effect of liquid crystals.

According to the continuum theory of liquid crystals, the elastic part of the internal energy density of a perturbed liquid crystal is given by the equation:

$$F_{def} = (1/2)\,[\,K_{11}\,(\nabla.\,\mathbf{n})^2 + K_{22}\,(\mathbf{n}.\,\nabla \times \mathbf{n})^2 + K_{33}\,(\mathbf{n} \times \nabla \times \mathbf{n})^2\,] \qquad 2.47$$

where the constants K_{11}, K_{22}, K_{33} are, respectively, termed as the splay, twist, and bend elastic constants and are named collectively known as the Frank elastic constants. **n** is the director. Furthermore, F_{def} must be positive in order to give stability for the uniformly aligned state, all the elastic constants (K_{11}, K_{22}, K_{33}) must be positive.

2.17 Freedericksz transition:

The elastic constants of the liquid crystals can be determined by various methods, of which Freedericksz transition is one of the simplest and convenient methods. The term Freedericksz transition refers to the deformation of a thin layer of nematic liquid crystal sample with a uniform director pattern in an external electric [68-71] or magnetic field [72-79]. Freedericksz observed that when a planar surface aligned nematic liquid crystal cell is subjected to magnetic field normal to the director then the cell undergoes an abrupt change in its optical properties if the strength of the external field exceeds the threshold value, known as the critical field. If the nematic liquid crystals have positive diamagnetic anisotropy or dielectric anisotropy, then as the field exceeds the critical value, the director starts to align along the external field. Depending on the geometry of the arrangement, we can determine, splay, twist or bend elastic constants

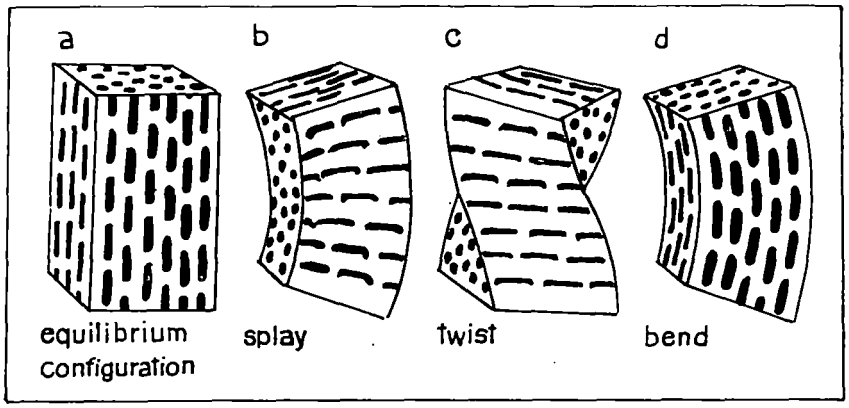

Figure 2.4. (a) An ordered liquid crystal in equilibrium configuration. The deformation states ---- (b) splay, (c) twist, (d) bend.

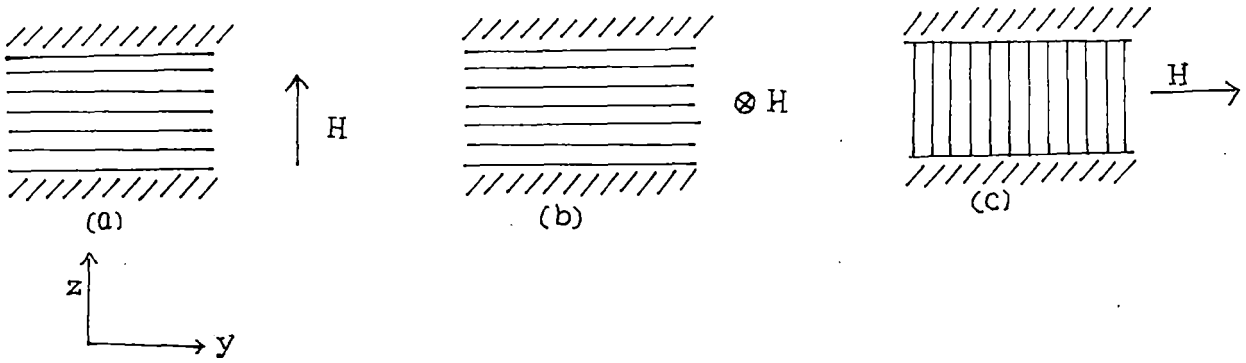

Figure 2.5 Schematic experimental set-up for the determination of the elastic constants from Freedericksz transition: (a) splay, (b) twist and (c) bend.

from Freedericksz transition in the magnetic field. It is shown schematically in Figures 2.4 and 2.5 respectively.

To explain the Freedericksz transition, I have considered a uniform planer layer i.e. is splay mode of nematogenic sample, and is shown in Figure (2.5a). Suppose the magnetic field is applied along the z-axis. When the field increases there is a gradual change in the director pattern once H exceeds a threshold value H_c. When $H < H_c$, the equilibrium state is shown in Figure 2.6(a) where the director is everywhere parallel to the y-axis. In this case a small fluctuation of the director will be damped because the stabilising elastic torque is greater than the de-stabilising magnetic torque. When $H > H_c$, the system will undergo transition to unstable equilibrium state whereby at the slightest fluctuation the system jumps to one of the two stable states as shown in Figures 2.6(b) and 2.6(d).

The threshold magnetic field for the splay, bend or twist deformation is related to the elastic constants by the equation:

$$(H_c)_i = (K_{ii} / \Delta\chi)^{1/2} \quad (\pi / d) \qquad 2.48$$

where d is the sample thickness, $\Delta\chi$ is the diamagnetic anisotropy and $(H_c)_i$ is the respective critical magnetic field.Also the subscript i =1,2,3. refers to the splay, twist and the bend deformation respectively.

2.18 Description of Experimental set-up for determination of K_{11} and K_{33}:

The apparatus of the determination of the elastic constants (K_{11} and K_{33}) has been designed and fabricated in our laboratory by M. K. Das and R. Paul [64]. The block diagram of the set-up has been shown in Figure 2.7.

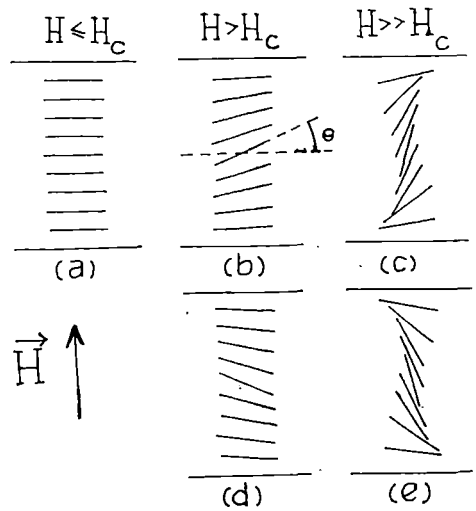

Figure 2.6. Schematic representation of the deformation of the director pattern when $H > H_c$ in the case of the splay mode.

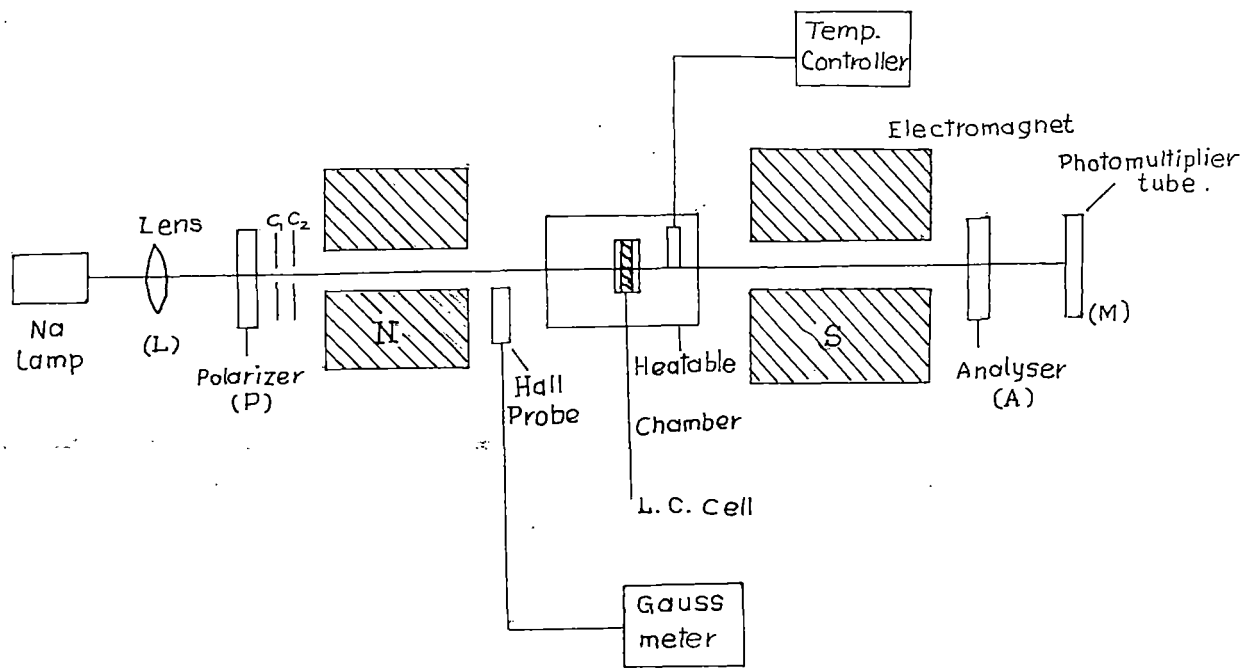

Figure 2.7 Schematic representation of the experimental set-up for elastic constant measurements.

The experimental sample was taken in a glass cell prepared from microscope slides. The cell was housed in a solid brass oven which has a groove at the proper angle and it also acts as a thermostat. The temperature was measured and controlled within an accuracy of $\pm 0.5\ ^0$C by means of a copper-constantan thermocouple inserted in the brass block and a temperature regulator (Indotherm model 457). A sodium D light was used as a source which was allowed to incident on the sample through a lens (L), polarizer (P) and collimating circular slits (C_1,C_2). The polarizer (P) and the analyser (A) were crossed at $\pm 45^0$ relative to the vertical axis. The transmitted light intensity was monitored by a photomultiplier tube (M) whose output was also measured by a nano-ammeter. The magnetic field was applied perpendicular to the director. For the Freedericksz transition to occur, the director must be truly oriented at right angle to the external field. In order to ensure this exact alignment, the brass oven was mounted on a specially constructed platform whose alignment with respect to the field could be adjusted to an accuracy of 1-2′ of arc. Further, the platform itself rested on levelling screws so that the alignment of the sample could be varied in every possible manner. The magnetic field intensity was varied slowly so that the nematic orientation remains in equilibrium with the applied magnetic field. The intensity of transmitted light was measured as the function of the applied magnetic field for any desired temperature. It was observed that when the field (H) exceeds a critical value (H_c) then there was an abrupt change in the optical properties of the sample. Thus we could measure the threshold field intensity (H_c) from the field versus intensity curve within an accuracy of $\pm$ 10 Gauss. The magnetic field was measured using a Hall-probe Gaussmeter (Model DGM-102).

The cell used in the experiment was made of two pieces of glass cut out from microscope slides with sides of 1 inch and 3/4 inch. The glass plates were cleaned by different cleaning agents and subsequently dried and treated for homeotropic or homogenous alignment as required. The smaller glass piece was centred on the larger piece separated by a thin glass-spacer of 150μm thickness. The actual thickness of the sample was measured by a microscope. The splay elastic constant (K_{11}) was measured by using homogenous planar aligned cell which was prepared by treating the inside surface of the glass plate with 1% aqueous solution of polyvinyl alcohol dried and then rubbed the layer in one direction with tissue paper. The bend elastic constant (K_{33}) was measured by using homeotropic cells which were prepared by the surface treatment of the glass plates with lecithin.

When the magnetic field intensity was increased beyond the critical value H_c, the transmitted light intensity exhibits oscillations due to the change of the phase retardation.

The threshold field for twist deformation cannot be detected optically when viewed along the twist axis. Due to the large birefringence of the medium for this direction of propagation, the state of polarisation of the transmitted beam is indistinguishable from that of the emerging beam from the untwist nematics. A total internal reflection technique can be used to measure the K_{22} values of the twist deformation. In my present work however, I have measured only K_{11} and K_{33} for ten different nematic liquid crystals.

Structure and chemical name of the liquid crystals studied:

The chemical names of the liquid crystals studied in the present investigation and their structural formula are given below:

1 & 2. 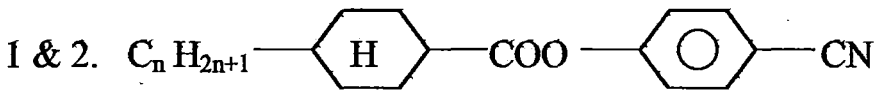

(i) n = 3, p-cyanophenyl trans- 4 - propyl cyclohexane carboxylate.
(CPPCC in short).

(ii) n = 4, p-cyanophenyl trans- 4 - butyl cyclohexane carboxylate.
(CPBCC in short).

3. 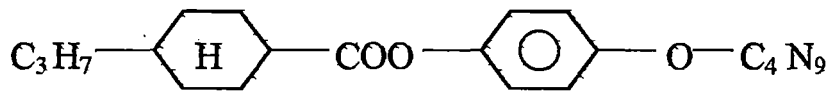

p- butoxyphenyl trans- 4 - propyl cyclohexane carboxylate.
(BPPCC in short).

4. 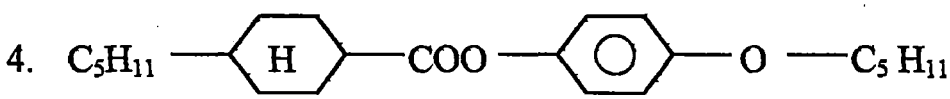

p- pentoxyphenyl trans- 4 - pentyl cyclohexane carboxylate.
(PPPCC in short).

5 & 6. 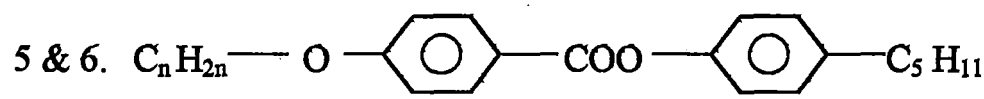

(i) n= 5, 4 -n-pentyl phenyl- 4 - n' pentyloxy benzoate.
(ME 5O.5 in short).

(ii) n= 6, 4 -n-pentyl phenyl- 4 - n' hexyloxy benzoate.
(ME 6O.5 in short).

7. 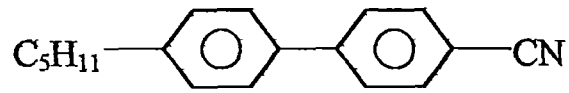

4 - n - pentyl - 4 - n'- cyanobiphenyl. (5CB in short).

8 & 9. 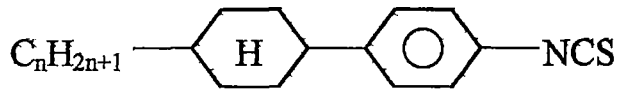

(i) n= 10, 4 - (trans - 4'- n- decyl cyclohexyl) isothiocyanatobenzene.
(10 CPS in short).

(ii)n=12, 4 - (trans - 4'- n- dodecyl cyclohexyl) isothiocyanatobenzene.
(12 CPS in short).

10. 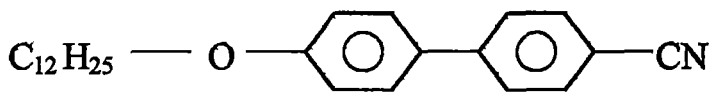

4 - dodecyloxy - 4'- cyanobiphenyl. (12OCB in short).

11. 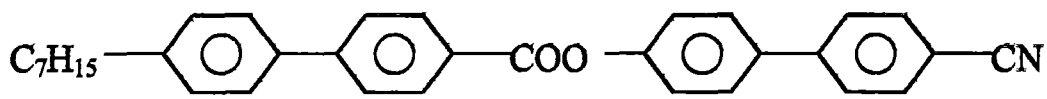

4 - cyanobiphenyl - 4'- yl - 4 - heptylbiphenyl - 4 - carboxylate.
(7CBB in short).

12 & 13. 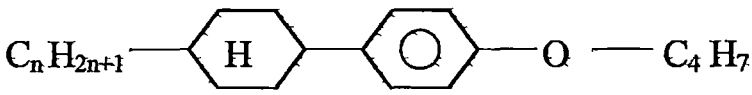

(i) n=3, 3E-n-butene-phenyl-(4-cyclohexane-4′-n-propane)-ether
{ 3CPOd (3)1 in short }

(ii) n= 5, 3E-n-butene-phenyl-(4-cyclohexane-4′-n-pentane)-ether
{ 5CPOd (3)1 in short }

The liquid crystals 1, 2, 3, 11 & 12 were obtained from Hoffmann-La Roche, Basel, Switzerland; the liquid crystals 4, 5 & 6 were obtained from E. Merck, UK; and the crystals 7, 8, 9 & 10 were donated by Prof. R. Dabrowski, Institute of Chemistry, Military University of Technology, Warsaw, Poland. All the samples were obtained in the pure state and were studied without further purification.

References:

1) E. B. Priestley, P. J. Wojtowicz and P. Sheng, Eds. Introduction to Liquid Crystals, Plenum, New York, (1974).
2) S. Chandrasekhar, Liquid Crystals, Cambridge University Press, Cambridge, (1977).
3) G. Vertogen and W. H. de Jue, Thermotropic Liquid Crystals, Fundamentals, Springer-Verlag (1988).
4) G. R. Luckhurst and G. W. Gray, (Editors) The Molecular Physics of Liquid Crystals, Academic Press (1979).
5) P. G. de Gennes, The Physics of Liquid Crystal, Clarendon Press, Oxford, (1974).
6) A. Saupe and W. Maier Z. Natureforsch, 14a, 882 (1959) and 15a, 287 (1960).
7) W. L. McMillan, Phys. Rev., A4, 1238 (1971).
8) W. L. McMillan, Phys. Rev., A6,936 (1972).
9) E. B. Priestley, P. S. Pershan, R. B. Meyer and D. H. Dolphin, Vijnana Parishad Anushandhan Patrika, 14, 93 (1971).
10) K. K. Kobayashi, J. Phys. Soc. (Japan), 29, 101 (1970).
11) K. K. Kobayashi, Mol. Cryst. Liq. Cryst., 13, 137 (1971).
12) D. Demus and L. Richter, Textures of Liquid Crystals, Verlag Chemie, New York (1978).
13) Advances in Liquid Crystals, Vol. 6, Ed. G. H. Brown, Academic Press (1983), Chapter 1.
14) B. K. Vainstein and I. G. Chistyakov, Problem of Modern Crystallography, Nauka, Moscow (1975).

15) A. J. Leadbetter, The Molecular Physics of Liquid Crystals, Eds. G. R. luckhurst & G. W. Gray, Chap.13, Academic Press (1979).

16) A. de Vries, Liquid Crystals, Ed. F. D. Saeva, M. Dekker Inc., NY.

17) A. J. Leadbetter and E. K. Norris, Mol. Phys., 38, 669 (1979).

18) A. de Vries, J. Chem. Phys., 56, 4489 (1972).

19) H. Kohli et al, Z. Physik, B24, 147 (1976).

20) A. de Vries, Mol. Cryst. Liq. Cryst., 10, 219 (1970).

21) P. S. Pershan, Structure of Liquid Crystal Phases, World Scientific (1988).

22) B. Jha and R. Paul, Proc. Nucl. Phys. Solid State Phys. Symp., India, 19c, 491 (1970).

23) C. Kittel, Int. to Solid State Physics, Wiley Eastern, Chap. 2 (1976).

24) H. P. Klug and L. E. Alexander, X-ray diffraction procedures, John Wiley and Sons, N.Y., p.114 and 473 (1974).

25) S. Ergun, J. Appl. Cryst., 1, 19 (1968).

26) R. Bruinsma and D. R. Nelson, Phys. Rev. B. , 23, 1, 402 (1981).

27) E. Gorecka, Li Chen, O. Lavrentovich and W. Pyzuk, Europhysics Letters, 27(7), 507, 1994.

28) R. J. Birgeneau and J. D. Litster, J. Phys. Letts., 39, L399, (1978).

29) B. K. Vainstein, Diffraction of x-rays by Chain Molecules, Elsevier Pub. Co. (1966).

30) R. Paul and G. Chaudhuri, Abstract in the 14th International Liquid Crystal Conference, Pisa, 1992, Abs.no.- H-P23.

31) E. Dorn, Z. Physik, 11, 111 (1910).

32) W. H. Pness, S. A. Teukolsky, W. T. Vellering and B. P. Flannery, Cambridge University Press, 1986, Chap. 15.

33) O. Weiner, S. Ber. Sachs. Ges. Wissensch., 61, 113 (1909).

34) H. Zocher, Naturwiss., 13, 1015 (1925).

35) H. Zocher, Z. Krist., 79, 122 (1931).

36) F. Grandjean, Compt. Rend., 168, 408 (1919).

37) N. V. Madhusudana, R. Sashidhar and S. Chandrasekhar, Mol. Cryst. Liq. Cryst., 13, 61 (1971).

38) Y. Poggi , J. Robert and J. Borel, Mol. Cryst. Liq. Cryst., 29, 31, (1975).

39) R. Chang, Mol. Cryst. Liq. Cryst., 30, 155 (1975).

40) C. C. Huang, R. S. Pindak and J. J. Ho, J. Phys. Lett. (Paris), 35, 185 (1974).

41) W. Kuczynski and B. Stryla, Mol. Cryst. Liq. Cryst., 31, 267 (1975).

42) M. Laurent and R. Journeaux, Mol. Cryst. Liq. Cryst., 36, 171 (1976).

43) G. Pelzl and H. Sackmann, Mol. Cryst. Liq. Cryst., 15, 75 (1971).

44) G. Pelzl and H. Sackmann, Symp. Faraday Soc., No. 5, 68 (1971).

45) Y. Galerne, S. T. Lagerwall and I. W. Smith, Opt. Commun., 19, 147 (1976).

46) H. E. Neugebauer, Canad. J. Phys., 32, 1 (1954).

47) M. F. Vuks, Optics and Spectroscopy, 20, 361 (1966).

48) A. Saupe and W. Maier, Z. Natureforsch, 16a, 816 (1961).

49) P. G. de Gennes, , Mol. Cryst. Liq. Cryst., 12, 193 (1971).

50) I. Haller, H. A. Huggins, H. R. Lilienthal and T. R. McGuire, J. Phys. Chem., 77, 950 (1973).

51) A. K. Zeminder, S. Paul and R. Paul, Mol. Cryst. Liq. Cryst. , 61, 191 (1980).

52) P. G. de Gennes, The Physics of Liquid Crystal, Clarendon Press, Oxford, p.31 (1974).

53) W. H. de Jue, Physical Properties of Liquid Crystalline Materials, Gordon Breach, NY, p. 24 (1980).

54) V. Tsvetkov, Acta Physicochim. USSR, 16, 132 (1942).

55) A. Saupe and W. Maier, Z. Natureforsch, 16a, 816 (1961).

56) J. P. Dias, C. R. Acad. Sci., Se'r, A282, 71 (1976).

57) J. O. Kessler, Liq. Cryst. Ord. Fluids, p. 361 (1970)

58) CRC Handbook of Chemistry and Physics, 58th edition, p.E-128. (1977- 78),

59) CRC Handbook of Chemistry and Physics, 58th edition, p.C-270 (1977- 78),.

60) A. Burris and C.D. Hause, J. Chem. Phys., 11, 442 (1943).

61) CRC Handbook of Chemistry and Physics, 58th edition, p. F-9. (1977- 78),

62)W. H. de Jue and W. A. P. Claassen, J. Chem. Phys., 68, 102 (1978).

63) M. Mitra and R. Paul, Mol. Cryst. Liq. Cryst., 148, 185 (1987).

64) M. K. Das and R. Paul, Mol. Cryst. Liq. Cryst., 259, 13 (1995).

65) H. Zocher, Trans Faraday Soc., 29, 945 (1933).

66) C. W. Oseen, Trans Faraday Soc., 29, 883 (1933).

67) F. C. Frank, Faraday Soc.Discussion, 25, 19 (1958).

68) H. Gruler, T. J. Schiffer and G. Meier, Z. Natureforsh, 27a, 966 (1972).

69) H. Gruler and L. Cheung, J. Appl. Phys., 46, 5097 (1975).

70) H. Deuling in Liquid Crystals, Solid State Physics Suppl. no. 14, ed. L. Liebert, Academic Press, NY, p. 77.

71) M. J. Bradshaw and E. P. Rayens, Mol. Cryst. Liq. Cryst., 72, 35 (1980).

72) V. Freedericksz and V. Tsvetkov, Phy. Z. Soviet Union, 6, 490 (1934).

73) V. Freedericksz and V. zolina, Trans. Faraday Soc., 29, 919 (1933).

74) P. P. Karat and N. V. Madhusudana, Mol. Cryst. Liq. Cryst., 40, 239 (1977).

75) H. P. Schad, M. A. Osman, J. Chem. Phys., 75 (2), 880 (1981).

76) F. Leenhouts, H. J. Boeber, A. J. Dekker and J. J. Jonker, J. Phys. (Paris) Colloque.,40, C3-291 (1979).

77) H. P. Schad, G. Bauer and G. Maier, J. Chem. Phys., 67, 3705 (1977).

78) F. Leenhouts and A. J. Dekker, J. Chem. Phys., 74, 1956 (1981).

79) H. P. Schad, M. A. Osman, J. Chem. Phys., 75 (2), 880 (1978).

80) L. Pohl and U. Finkenzeller in B. Bahadur (Ed.) Liquid Crystals, Application and Uses, Vol. 1, World Scientific, p. 166 (1990)